

The properties of thin ^3He - ^4He superfluid films

R.H.Anderson, M.D.Miller

Department of Physics, Washington State University,
Pullman, WA 99164-2814 USA

Received August 11, 2000

Thin ^3He - ^4He physisorbed films are examples of strongly interacting, quasi two-dimensional, fermion-boson mixture systems. The properties of the mixture systems can be tuned by changing the substrate or the ^4He film thickness. In this paper, we discuss the ground-state and magnetic ground-state of the ^3He subsystem and also the interactions between the excitations of the ^4He superfluid film with the single-particle excitations of the adsorbed ^3He . The ground-state of the ^3He system is calculated using a model for the ^3He - ^3He effective interaction in the static ^4He film which explicitly includes the effective interaction due to exchange of virtual film excitations (rippions). This latter effective interaction is evaluated in the random phase approximation and is shown *not* to be capable of causing the ^3He system to be self-bound. We discuss the evidence from magnetization, third sound and heat capacity measurements that the ^3He first transverse excited state is being occupied prior to monolayer completion.

Key words: *superfluid films, ^3He - ^4He mixtures, third sound, ripples*

PACS: *67.70.+n, 67.60.Fp, 64.30.+t*

1. Introduction

In recent years, there has been considerable effort in trying to understand the properties of ^3He - ^4He mixture films [1]. There have been surprises along the way. One of the most interesting was the realization that in these thin films the ^3He transverse excited states are occupied at *submonolayer* coverages. The occupation of these states affects the equation of state, the hydrodynamic response and the response to magnetic and thermal probes. In this paper we shall discuss first excited state occupation both from the point of view of a semi-phenomenological microscopic calculation and also an analysis of existing magnetization data. We shall also discuss recent third sound experiments and the role that they play in this analysis. The first attempt to examine the transverse bound state structure of a single ^3He atom in a ^4He superfluid film was reported by Gasparini *et al.* [2]. These authors adapted

the Lekner [3] type of approach developed by Mantz and Edwards [4] for the bulk ^4He surface. For ^4He films of 13.0 Å and 15.3 Å thickness they found that the level spacing from the ground-state to the first excited state, Δ , was 2.88 K and 2.76 K respectively. If the ^3He is modeled as an ideal quasi-particle gas with effective mass m_3^* , then the value of the ^3He areal density, σ_3 , when the Fermi energy is equal to the level spacing is given by $\sigma_{3F} = (\Delta m_3^*/\pi\hbar^2)$. If we use $m_3^* = 1.38m_3$, the hydrodynamic effective mass, then the level spacings calculated in [2] correspond to densities of 0.079 Å⁻² and 0.076 Å⁻², respectively. The conventional areal density corresponding to monolayer completion, $\sigma_{\text{max}} = (n_3^o)^{2/3} = 0.065 \text{ Å}^{-2}$, where $n_3^o = 0.0165 \text{ Å}^{-3}$ is the bulk ^3He number density. Thus the results of [2] predict that, at temperatures low relative to the Fermi energy, there should be no ^3He occupation of the first transverse excited state before monolayer completion.

Sherrill and Edwards [5] used a more elaborate version of the Mantz and Edwards theory [4] where some adjustable parameters used in [2] were eliminated. They calculated the ground-state and first excited state energies as a function of film thickness and showed that for thin ^4He films the influence of the substrate van der Waals potential is important. For thin films, the attractive substrate potential causes both the ground-state and first excited state energies to decrease rapidly. The ground-state decreases faster than the first excited state and so the level spacing *increases* as the film becomes thinner. Anderson and Miller [6] using a semi-phenomenological effective interaction for the ^3He in the film also calculated the ground-state and excited state energies as a function of film thickness and found, in agreement with [5], that the level spacing increases with decreasing film thickness. We note that the value of the level spacing when $\sigma_{3F} = \sigma_{\text{max}}$ is $\Delta_F = 2.4 \text{ K}$ which is quite close to the spacing of the ^3He surface state on bulk ^4He relative to the ^3He chemical potential in bulk ^4He (2.22 K). For $\Delta > \Delta_F$ we expect no occupation of the first excited state before the first monolayer is completed. The results of the single-particle calculations, [5] and [6], thus indicate that for thin ^4He films there should be no occupation of the first excited state prior to monolayer completion

In the most elaborate set of calculations of the single- ^3He properties in a ^4He film to date, Krotscheck, Saarela and Epstein [7] solved a coupled variational problem for both the film and the adatom in the substrate potential. The major difference between their system and those considered in [5] and [6] is that the ^4He film took on realistic transverse structure and was not simply treated as a slice of the bulk. For the thinnest film that they studied, they reported a level spacing $\Delta = 3.09 \text{ K}$. This means $\sigma_{3F} = 0.085 \text{ Å}^{-2}$ which once again predicts that the first excited state will not be reached before monolayer completion.

On the experimental side, Higley, Sprague and Hallock [8] using magnetization measurements on a mixture film system adsorbed on Nuclepore filter, showed unambiguously that, for this substrate, the ^3He is promoted to the first excited state at coverages far less than a completed monolayer. These results were confirmed in third sound measurements by Sheldon and Hallock [9] as pointed out by Anderson, Miller and Hallock [10]

In section 2, we shall give a brief overview of the ground-state theory as developed

by Anderson and Miller [6,11]. In [11], Anderson and Miller generalized the approach in [6] to include the presence of ${}^3\text{He}$ transverse excited states. One product of this approach was a density dependent level spacing, Δ , due to the effective interaction between ${}^3\text{He}$ atoms and due to the exchange of virtual film excitations, ripples, and is denoted by the one ripplon exchange potential (OREP). The value of Δ decreased with increasing ${}^3\text{He}$ coverage thus providing theoretical support for the experimental observation that first excited state occupation occurs prior to monolayer completion.

We note that an alternative way to view this mechanism is from Landau's Fermi-liquid theory. The OREP contributes to the residual ${}^3\text{He}$ - ${}^3\text{He}$ quasiparticle interaction. This may yield an effective mass, m_3^* , with strong density dependence. Then one would interpret a density dependent level spacing as simply the manifestation of the density dependence in the effective mass. Calculations of the Fermi-liquid parameters are in progress [12].

In section 3, we shall give a brief description of the magnetization measurements and, in the ideal quasi-particle limit, derive the coverage dependence of the excited state population. In section 4, we discuss the effects of the ${}^3\text{He}$ transverse state occupation on third sound, the ${}^4\text{He}$ film's hydrodynamic modes. Section 5 is the conclusion.

2. ${}^3\text{He}$ ground-state (the OREP)

We consider a film with N_4 ${}^4\text{He}$ atoms and N_3 ${}^3\text{He}$ atoms which is physisorbed to some solid substrate which occupies the lower half space ($z \leq 0$). The ${}^4\text{He}$ film occupies area A and, in equilibrium, is laterally transitionally invariant. The film has thickness d . (d can be defined as the height of a mobile layer above the substrate surface as measured in a third sound experiment.)

The model Hamiltonian [6,11] can be written

$$H = H_4 + H_3 + H_{34}, \quad (2.1)$$

where

$$H_4 = \sum_{\mathbf{k}} \hbar \Omega_k \left[b_{\mathbf{k}}^\dagger b_{\mathbf{k}} + \frac{1}{2} \right], \quad (2.2)$$

$$H_3 = \sum_{\mathbf{k}, \mu} \epsilon_{\mathbf{k}, \mu} a_{\mathbf{k}, \mu}^\dagger a_{\mathbf{k}, \mu}, \quad (2.3)$$

$$H_{34} = \frac{1}{\sqrt{A}} \sum_{\mathbf{k}, \mathbf{m}} (\Gamma_{\mathbf{m}}^{\mu\nu} a_{\mathbf{k}+\mathbf{m}, \mu}^\dagger a_{\mathbf{k}, \nu} b_{\mathbf{m}} + \Gamma_{-\mathbf{m}}^{\mu\nu} a_{\mathbf{k}, \mu}^\dagger a_{\mathbf{k}+\mathbf{m}, \nu} b_{\mathbf{m}}^\dagger). \quad (2.4)$$

H_4 , equation 2.2, is the ${}^4\text{He}$ film Hamiltonian. The frequencies, Ω_k are third sound/capillary wave modes and are defined in [6,11]. H_3 is the Hamiltonian for a noninteracting ${}^3\text{He}$ system embedded in the ${}^4\text{He}$ background. The ${}^3\text{He}$ single particle states can be factored into a lateral, quasi-continuum of plane waves times

transverse, discrete single-particle states. Thus the energies can be written:

$$\epsilon_{\mathbf{k},\mu} = \frac{\hbar^2 k^2}{2m_3^*} + \epsilon_\mu, \quad (2.5)$$

where the ϵ_μ are the eigenenergies of a single-particle-like Schrödinger equation:

$$-\frac{\hbar^2}{2m_3^*} \varphi_\mu''(z) + v_3(z) \varphi_\mu(z) = \epsilon_\mu \varphi_\mu(z). \quad (2.6)$$

$v_3(z)$ is the single particle, effective interaction due to the substrate and background ^4He film. H_{34} , equation 2.4, is the lowest order ^3He - ^4He interaction. The vertex functions, $\Gamma_{\mathbf{m}}^{\mu\nu}$, for the ^3He -ripplon scattering between transverse states labelled by the superscripts, are determined by matrix elements for a model of the ^3He - ^4He effective interaction. The single particle effective interaction, $v_3(z)$, introduced in equation 2.6 is determined by the same model effective interaction. Such a model is introduced and discussed in detail in [6,11]. In figure 1 we illustrate the vertex function $\Gamma^{00}(q)$ calculated for a ^4He film thickness of 12.3 Å.

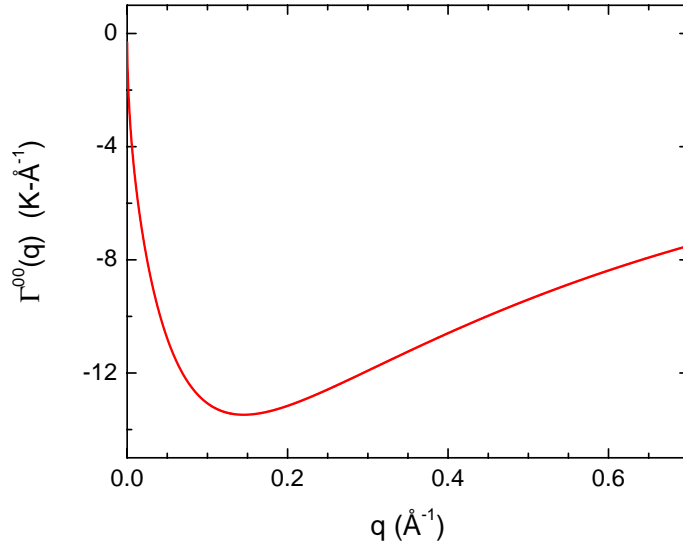


Figure 1. The vertex function $\Gamma^{00}(q)$ calculated as described in [6] for a ^4He film of thickness 12.3 Å.

Utilizing standard equation of motion methods [6] it is straightforward to determine from equation 2.4 the third-sound-mediated ^3He - ^3He interaction (the OREP). The OREP is given by

$$V_{\text{OREP}}^{\alpha\gamma\beta\delta}(q, \omega) = \frac{\Gamma^{\alpha\beta}(q) \Gamma^{\gamma\delta}(-q)}{\hbar} \left[\frac{1}{(\omega - \Omega_q + i\eta)} - \frac{1}{(\omega + \Omega_q - i\eta)} \right], \quad (2.7)$$

where, as above, the $\Gamma^{\alpha\beta}(q)$ are the vertex functions, and the quantity in square brackets is the (time-ordered) free ripplon propagator.

In [11], we combined the OREP with an effective *direct* ^3He - ^3He interaction (a softened Lennard-Jones) to compute the ground-state energy and free energy in the thermal Hartree Fock approximation. The energy showed no sign of a van der Waals loop which we interpreted as indicating that *no gas-to-liquid transition has occurred*.

In the equation of state calculations described above only the static limit of the OREP was used. In recent work [13,14] which we shall describe below, we have investigated the contribution to the ground-state energy from the fully frequency dependent OREP in the random phase approximation (RPA). The zero temperature RPA contribution to the ground-state energy of a 2D fermion system is given by [15]

$$\Delta E_{\text{RPA}} = -\frac{i}{2} \frac{A\hbar}{(2\pi)^3} \int d^2q \int_{-\infty}^{+\infty} d\omega \left\{ \ln [1 - V(q, \omega) \Pi^0(q, \omega)] + V(q, \omega) \Pi^0(q, \omega) \right\}, \quad (2.8)$$

where \mathbf{q} is the 2D momentum, ω is the frequency, $V(q, \omega)$ is the Fourier transform of the interaction potential, $\Pi^0(q, \omega)$ is the 2D free fermion polarization propagator, and A is the area of the system. The potential used in this calculation is the OREP given by equation 2.7.

The RPA energy comes from the imaginary part of the integral as seen by the presence of the factor i in front of the integral. The linear (nonlogarithmic) term in equation 2.8 can be evaluated by straightforward numerical integration. We note that the imaginary part of V_{OREP} has Dirac delta-functions which pin the frequency to the ripplon frequency or its negative.

The logarithmic term was evaluated for a finite box model of the fermion system. A square box of length L such that $A = L^2$ was chosen. The polarization propagator then becomes a discrete sum over a finite number of single pole terms which are equally spaced along the real ω axis. Consecutive poles are spaced by the separation, $\Delta\omega$, where $\Delta\omega = (2\pi\hbar/mL)q$. Consequently the argument of the logarithm, $1 - V(q, \omega) \Pi^0(q, \omega)$, assumes an analytic structure similar to that of the polarization propagator. The ω integral of the logarithmic term accumulates an imaginary value whenever the real value of the logarithm is negative. The imaginary value of the logarithm is either $+i\pi$ or $-i\pi$ according to whether the branch cut is approached from above or below the real ω axis as determined by the infinitesimal imaginary part of the denominator in the propagator. The integral of the logarithmic term becomes, therefore, the product of $\pm i\pi$ and the sum of the segments of the ω -axis, $\delta_i\omega$, for which $\text{Re}\{V_{\text{OREP}}(q, \omega) \Pi^0(q, \omega)\} \geq 1$. The logarithmic term in the RPA energy can be written

$$\pm \frac{1}{2} \left(\frac{\hbar}{2\pi} \right) \sum_{\mathbf{q}} \sum_{\text{poles}} \pi \delta_i\omega. \quad (2.9)$$

The sum of the $\delta_i\omega$ segments reduces to a compact formula in the limit of large area, A , of the normalization box. We note that the i subscript labels a particular

pole in the polarization propagator. The final form for the logarithmic contribution to the RPA energy, after symmetry of the ω -dependence is considered, can be written as

$$\left(\frac{\hbar}{2\pi}\right) \sum_{\mathbf{q}} \sum_{\omega_i > 0} \tan^{-1} \left[\frac{2\pi\eta_i V_{\text{OREP}}(q, \omega)}{A\hbar\Delta\omega} \right] \Delta\omega. \quad (2.10)$$

The quantity η_i is a degeneracy factor which counts the number of states which yield identical contributions to the frequency integral for a given value of the wavevector \mathbf{q} . Explicit expressions for the degeneracy factors can be found in [14]. We note that in the limit $L \rightarrow \infty$ the degeneracy factor per unit length, η_i/L , is nearly the same for the i^{th} pole and its neighbouring terms. The final form shown for equation 2.10 is obtained by treating η_i as a common multiplier.

The contribution of this expression was obtained numerically. Successively greater values were assigned to the box length L until further increase did not alter the first two significant figures. A value of L on the order of a few thousand Angstroms was found to be sufficient.

There is one additional contribution to the RPA energy which we have not mentioned yet and it is *only* present for a potential whose real part is positive. For V_{OREP} , in the asymptotic frequency regime beyond the last pole, *i.e.* $\omega > \omega_{\text{max}}$, there is a zero sound contribution for frequencies greater than the ripplon frequency, $\omega > \Omega_q$. There are two cases to consider $\Omega_q < \omega_{\text{max}}$ and $\Omega_q > \omega_{\text{max}}$. These are discussed in [14].

For the numerical results to be discussed below, we use the transverse, ground-state matrix elements for $V_{\text{OREP}}(q, \omega)$. That is, we set $\alpha = \beta = \gamma = \delta = 0$ in equation 2.7. Thus this model calculation is only strictly valid for the density regime below the onset coverage for first excited state occupation. For a 3.67 layer superfluid ^4He film on a Nuclepore substrate, the first excited ^3He transverse state begins to be occupied at a coverage of 0.6 monolayers ($\approx 0.04 \text{ \AA}^{-2}$).

In figure 2, we show the RPA energy per particle as a function of ^3He density for V_{OREP} with its full frequency dependence and also in the static limit. We note that frequency dependence may have an important effect on the magnitude of the correlation energy. In the density range of interest, the RPA energy obtained with the static V_{OREP} is always negative and less than the RPA energy obtained with the dynamic V_{OREP} . Indeed, the inclusion of explicit frequency dependence in the potential causes the RPA energy to be positive in the density range of interest. We note that neither set of results has appreciable density dependence.

Finally we note the importance of using the time ordered form for $\Pi^0(q, \omega)$. This is especially clear for a real static potential where the product $V(q) \text{Im} \Pi^0(q, \omega)$ is an even function of ω for the time ordered propagator but is odd for the retarded form.

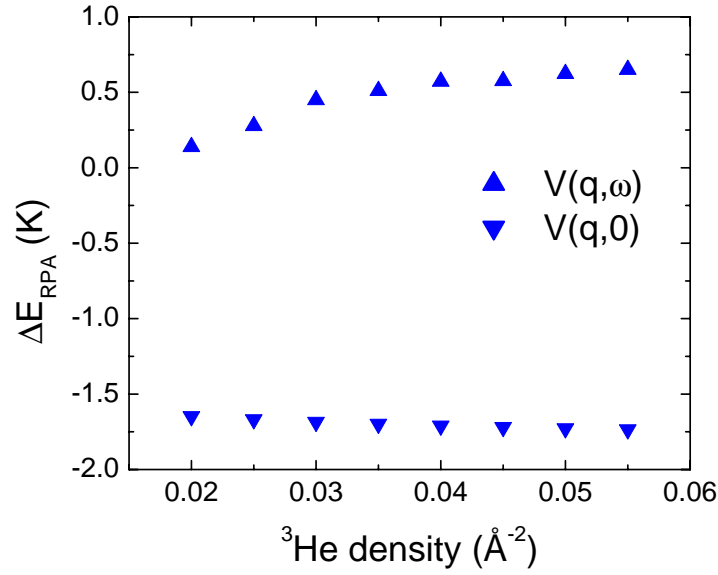


Figure 2. The RPA energy for the OREP as a function of density. The upper results are for the fully frequency dependent V_{OREP} and the lower results are for the static limit as discussed in the text.

3. ^4He film excitations: third sound

In [16,17], it was shown that the expression for third sound in a ^3He - ^4He mixture film at very low temperatures is given by

$$\left(\frac{c_3^2}{c_{3o}^2}\right)_{\text{cont. growth}} = 1 - \frac{n_3^o}{n_4^o} \left[1 - \left(1 + \frac{h_u}{h_4}\right)^{-4} \right], \quad (3.1)$$

where n_3^o and n_4^o are the bulk ^3He and ^4He number densities, respectively and the quantity $c_{3o}^2 = -(h_4 - h_o) f_\ell(h_4)$ is the third sound speed for pure ^4He . This is a two layer model where the ^3He is confined to the upper film of thickness h_u and the superfluid ^4He is in the lower mobile layer of thickness $h_4 - h_o$. h_o is the thickness of the first immobile layers near the solid substrate.

For almost all of the data reported in [16], the ^3He upper films were greater than a monolayer and so adding ^3He to the system simply increases h_u in a continuous manner. For a continuous growth model, all of the information concerning changes in the third sound speed due to the addition of ^3He to the system is contained in the magnitude of h_u . For submonolayer ^3He , this model may not be sensible. Adding ^3He atoms in that case changes the areal density in the surface ground-state but does not affect the “thickness” of the film, a quantity which is fixed by the transverse extent of motion of the adsorbed ^3He atom. If we try to take account of the quantum mechanical transverse motion of the ^3He atom from the beginning then we are led to a picture different from a classical continuous growth model. We can imagine a

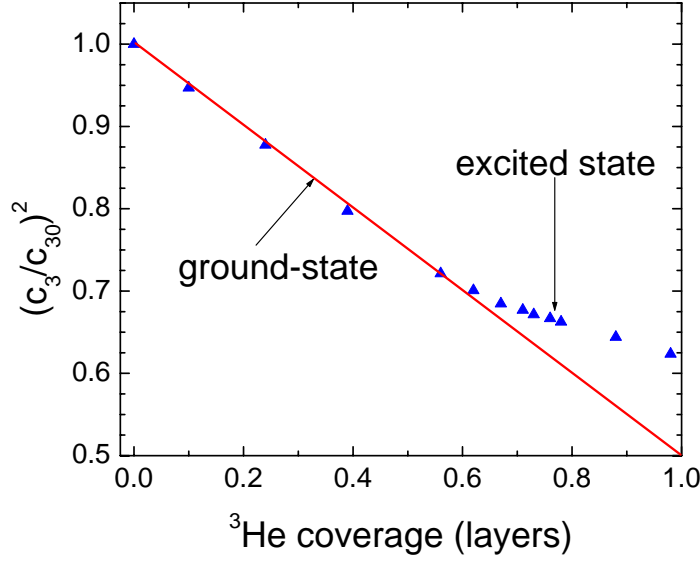


Figure 3. Third sound squared as a function of ${}^3\text{He}$ coverage. The triangles are the data of Sheldon and Hallock [9] and the line is the ground-state theory of equation (3.2). The change in slope at a coverage of 0.6 is the onset of excited state occupation.

“box” of area A and thickness h_u . As ${}^3\text{He}$ is added to this “box” the only effect at low densities is to change the ratio of the mass density in the upper film to that of the lower film.

Thus, in this picture, we find [10]:

$$\left(\frac{c_3^2}{c_{30}^2}\right)_o = 1 - \Delta_{\ell_o}\theta_3, \quad (3.2)$$

where $\theta_3 = (\sigma_3/\sigma_{3\text{max}})$ is the coverage in units of monolayers, $\sigma_{3\text{max}} = (n_3^o)^{\frac{2}{3}} \approx 0.065 \text{ \AA}^{-2}$ is the areal density at monolayer completion, and the slope is given by

$$\Delta_{\ell_o} = \frac{n_3^o}{n_4^o} \left[1 - \left(1 + \frac{h_u}{h_4} \right)^{-4} \right]. \quad (3.3)$$

In the low coverage regime where the ${}^3\text{He}$ only occupies the transverse ground-state, c_3^2/c_{30}^2 should be a linearly decreasing function of the coverage with a slope given by equation (3.3). We note that the slope Δ_{ℓ_o} depends only on the thickness of the superfluid film and is *independent of the substrate*.

In figure 3 we compare equation (3.2) with the experimental data of Sheldon and Hallock [9]. In this system, $h_4 = 3.67\ell_4$, and $\ell_4 = (n_4^o)^{\frac{1}{3}} = 3.6 \text{ \AA}$, is the thickness of one ${}^4\text{He}$ monolayer. Excellent agreement with the experimental data is obtained by fixing the parameter $h_u = 3.9 \text{ \AA}$. The parameter h_u is a measure of the thickness of

the ${}^3\text{He}$ transverse ground-state probability density and we note in passing that this particular value for h_u is the conventional ${}^3\text{He}$ layer thickness ℓ_3 , where $\ell_3 = (n_3^0)^{\frac{1}{3}} = 3.9 \text{ \AA}$. Thus, with $h_u = \ell_3$, we find $\Delta_{\ell_0} = 0.5$, which is in excellent agreement with the experimental data. We note that the continuous growth model also shows a linear decrease in c_3^2 with increasing coverage in the low coverage limit. In that case the slope is given by $\Delta_{\text{cont. growth}} = (4\sigma_{3\text{max}}/n_4^0 h_4)$, and for the system of [9], $\Delta_{\text{cont. growth}} \simeq 0.9$, nearly a *factor of two* in disagreement with experiment.

The third sound experimental data in figure 3 shows a change in slope at a coverage ≈ 0.6 . We interpret this change in slope as the signal of the onset of occupation of the first excited state. The fact that the slope bends up in figure 3, that is, the third sound speed increases relative to what the third sound speed would be if all the ${}^3\text{He}$ were in the ground state, is an important constraint on models for third sound in this region. A second constraint, as will be discussed in section 4, comes from an analysis of the magnetization step data of [8,18,19].

There have been a number of calculations of the wave functions for the ${}^3\text{He}$ transverse excited states [5–7]. The first excited state wavefunction has a larger transverse extent than the ground-state, which we interpret as a larger value for the parameter h_u . The change in the value of h_u affects the third sound speed in two ways. First, by increasing the thickness of the normal fluid layer, the third sound speed is decreased. Second, by decreasing the mass density in the normal fluid layer, the third sound speed increases. For agreement with experiment, the latter effect must dominate the former.

4. ${}^3\text{He}$ transverse excitations: magnetization

In [12] a simple ideal quasi-particle picture is introduced to explain the magnetization steps of [8,18,19]. We apply a uniform magnetic field of strength H_0 . The quasiparticle energies are given by

$$\begin{aligned}\varepsilon_{0\uparrow} &= \varepsilon_0^0 + \frac{\hbar^2 k^2}{2m_0^*} - \mu_N H_0, \\ \varepsilon_{0\downarrow} &= \varepsilon_0^0 + \frac{\hbar^2 k^2}{2m_0^*} + \mu_N H_0,\end{aligned}\tag{4.1}$$

where $\mu_N = \frac{1}{2}g\beta$, g is the Landé g-factor and $\beta = e\hbar/2mc$ is the Bohr magneton. The subscript 0 on the ε 's and the m^* labels the transverse ground-state. The first ${}^3\text{He}$ atoms added to the system will have their spins polarized up. When the highest energy spin-up particle is $2\mu_N H_0$ above the bottom of the band then the spin-down Fermi sea will begin to populate. Suppose that this occurs at wavevector $k = k_{L0}$, the number density in the spin-up band is $\sigma_{L0} = k_{L0}^2/4\pi$. Equating $\varepsilon_{0\uparrow}$ with $\varepsilon_{0\downarrow}$ at $k = k_{L0}$ then yields $\sigma_{L0} = m_0^* \mu_N H_0 / (\pi \hbar^2)$. The total magnetization, M_0 , is given by

$$M_0 = \frac{m_0^* \mu_N^2 H_0 A}{\pi \hbar^2}.\tag{4.2}$$

Increasing the density will now populate both the spin-up and spin-down transverse ground-state Fermi seas. Thus, the magnetization will be unchanged in this region and we will form the first step. This continues until the spin-up band of the first excited state is reached. Thus at $k = k_{R\uparrow}$ we have $\varepsilon_{0\uparrow} = \varepsilon_{1\uparrow}$ and at $k = k_{R\downarrow}$ we have $\varepsilon_{0\downarrow} = \varepsilon_{1\uparrow}$. These yield

$$\frac{\hbar^2 k_{R\uparrow}^2}{2m_0^*} = \Delta, \quad (4.3)$$

$$\frac{\hbar^2 k_{R\downarrow}^2}{2m_0^*} = \Delta - 2\mu_N H_0, \quad (4.4)$$

where we have defined $\Delta = \varepsilon_1^0 - \varepsilon_0^0$, the single particle level spacing. If we add these together we find

$$\frac{\hbar^2 (2\pi\sigma_{R0})}{2m_0^*} = \Delta - \mu_N H_0, \quad (4.5)$$

where $\sigma_{R0} = (k_{R\uparrow}^2 + k_{R\downarrow}^2) / 4\pi$ and the R (L) subscript refers to the right (left) hand limit of the magnetization step. We note that in the absence of an external field, the first excited state would begin to be filled at an onset density σ_{onset} given by

$$\frac{\hbar^2 (2\pi\sigma_{\text{onset}})}{2m_0^*} = \Delta. \quad (4.6)$$

If we substitute σ_{L0} and (4.6) into equation (4.5) we immediately find

$$\sigma_{\text{onset}} = \sigma_{L0} + \sigma_{R0}. \quad (4.7)$$

Thus the sum of the densities at the beginning and end of the magnetization step gives the onset density for first excited state occupation in *no external field*.

Thus as with the ground-state, the magnetization will continue to increase linearly with the ^3He density until the bottom of the spin-down Fermi sea is reached. The total magnetization at that point can be written $M = M_0 + M_1$, where

$$M_1 = \frac{m_1^* \mu_N^2 H_0 A}{\pi \hbar^2}. \quad (4.8)$$

Thus the increase in the magnetization per unit area before each step is proportional to the effective mass of the last state that is being filled. If the effective masses are equal then the magnetization steps are the same size.

Finally, for the ideal gas we can calculate the fractional filling of the first excited state in terms of the effective masses. Thus, in zero external field, if the density $\sigma > \sigma_{\text{onset}}$ then

$$x_1 = \frac{N_1}{N} = \frac{(1 - \sigma_{\text{onset}}/\sigma)}{(1 + m_0^*/m_1^*)}. \quad (4.9)$$

In the case $m_0^* = m_1^*$, then $x_1 = \frac{1}{2} (1 - \sigma_{\text{onset}}/\sigma)$ as used previously in [10] and [20].

5. Conclusion

It was argued by Miller and Nosanow [21] that pure two-dimensional ^3He should be a gas down to absolute zero. In the ^4He medium, however, the OREP provides a mechanism by which the ^3He subsystem could undergo a gas to liquid transition. In this paper we have summarized a new, numerically-based method to calculate the contribution to the ground-state energy in the RPA of the OREP [18]. We have concluded that the OREP even with full frequency dependence *does not* provide a mechanism for self-binding of the ^3He .

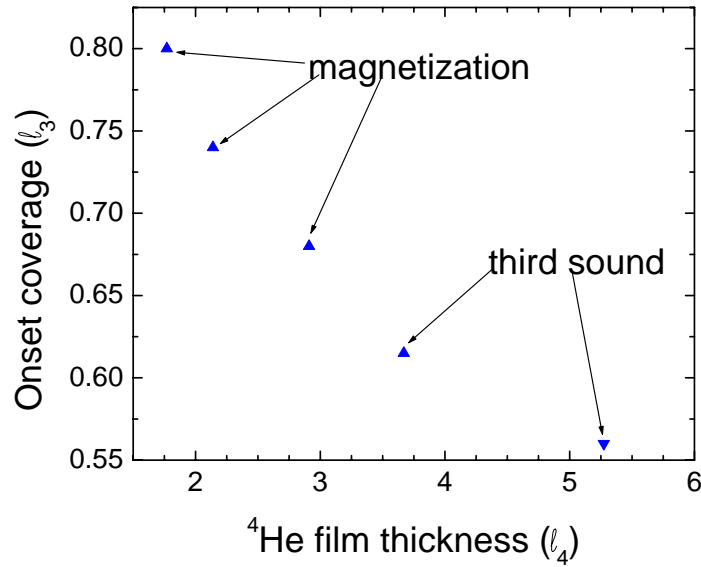


Figure 4. Onset coverage for first excited state occupation as a function of ^4He film thickness. The three low coverage points are from the analysis of the magnetization data as discussed in the text. The point at $3.67l_4$ is taken from figure 1. The upside-down triangle at $5.274l_4$ is an uncertain lower limit determined by an unpublished third sound run.

In figure 4 we plot θ_{onset} , the onset coverage, obtained from the three magnetization experiments together with the value obtained from figure 1, for the third sound analysis at $3.67l_4$. The magnetization data are from measurements made at three ^4He film thicknesses: $1.77l_4$, $2.14l_4$, and $2.91l_4$ [1,18]. The onset coverages are determined by an analysis based on equation 4.7. The fit is quite consistent. The decrease in the onset coverage as a function of increasing ^4He film thickness is due to the increase in the level spacing, Δ , with *decreasing* film thickness. The above analysis yields $\Delta \approx 1.9$ K, 1.8 K, 1.7 K for the three films, respectively. [For these results we use $m_3^* = 1.38m_3$ the hydrodynamic effective mass.] These spacings are in agreement with the measured values of Alikacem, Sprague and Hallock [18]. We note that there is both experimental, [2], and theoretical, [11], evidence that Δ seems to be a function of θ_3 in addition to h_4 . We note that in a heat capacity

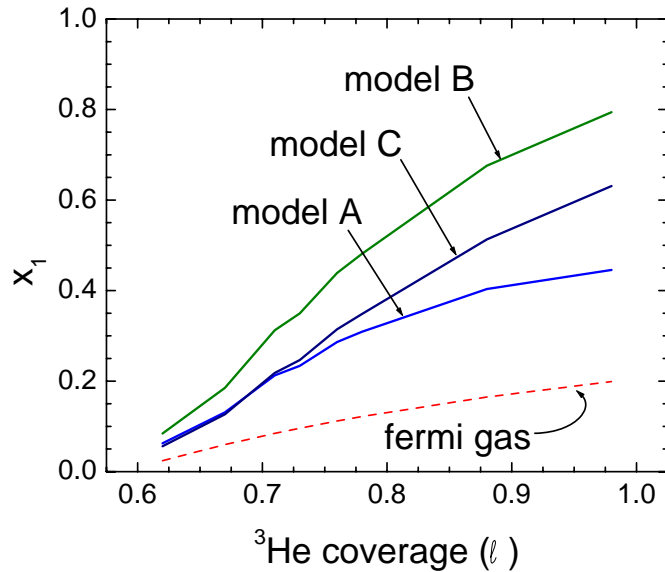


Figure 5. First excited state fractional population as a function of ${}^3\text{He}$ coverage. The line labelled *fermi gas* is from equation 4.9. *Model A*, *Model B* and *Model C* are models for the third sound speed as a function of different assumptions concerning the spatial distribution of ${}^3\text{He}$ in the first transverse excited state [20].

measurement made as a function of ${}^3\text{He}$ density at fixed temperature, occupation of the first excited state will be seen as a step increase in the heat capacity. This behaviour has been observed by the London group [22] in submonolayer ${}^3\text{He}$.

A detailed analysis of the third sound speed in the mixture film was given in [20]. A theory to explain the change in the third sound speed, as shown in figure 1, after the first transverse excited state begins to be populated, requires fairly detailed knowledge of the spatial distribution of the ${}^3\text{He}$ in the excited state *in the presence* of a dense system in the ground-state. Thus, this is a very nontrivial quantum many-fermion problem. In [20], we introduced three plausible models for the ${}^3\text{He}$ distribution and then used the experimental third sound speeds to solve for the fractional population of ${}^3\text{He}$ in the first excited state as a function of ${}^3\text{He}$ coverage. In figure 5, we compare these results with the ideal quasi-particle result of equation 4.9. We note that the third sound models yield first excited state populations that are larger than the ideal fermi gas model; however, the basic shapes of these curves are quite similar to one another. Please see [20] for a detailed discussion.

Acknowledgements

The research described in this publication was made possible in part by Award No. UW0-1012 of the U.S. Civilian Research and Development Foundation for Independent States of the Former Soviet Union (CRDF).

References

1. Hallock R.B. – In: Progress in Low Temperature Physics, Vol. XIV, edited by W.P.Halperin (Elsevier North Holland, Amsterdam, 1995), p. 321 and references cited therein.
2. Gasparini F.M., Bhattacharyya B., DiPirro M.J. // Phys. Rev. B, 1984, vol. 29, p. 4921.
3. Lekner J. // Philos. Mag., 1970, vol. 22, p. 669.
4. Mantz I.B., Edwards D.O. // Phys. Rev. B, 1979, vol. 20, p. 4518.
5. Sherrill D.S., Edwards D.O. // Phys. Rev. B, 1985, vol. 31, p. 1338.
6. Anderson R.H., Miller M.D. // Phys. Rev. B, 1989, vol. 40, p. 2109.
7. Krotscheck E., Saarela M., Epstein J.L. // Phys. Rev. B, 1988, vol. 38, p. 111.
8. Higley R.H., Sprague D.T., Hallock R.B. // Phys. Rev. Lett., 1989, vol. 63, p. 2570.
9. Sheldon P.A., Hallock R.B. // Phys. Rev. B, 1994, vol. 50, p. 16082.
10. Anderson R.H., Miller M.D., Hallock R.B. // Phys. Rev. B, 1999, vol. 59, p. 3345.
11. Anderson R.H., Miller M.D. // Phys. Rev. B, 1993, vol. 48, p. 10426.
12. Anderson R.H., Krotscheck E., Miller M.D. (unpublished).
13. Anderson R.H., Miller M.D. – In: Proceedings of Quantum Fluids and Solids, 2000.
14. Anderson R.H., Miller M.D. (preprint).
15. Fetter A.L., Walecka J.D. Quantum Theory of Many-Particle Systems. New York, McGraw-Hill, 1971.
16. Ellis F.M., Hallock R.B., Miller M.D., Guyer R.A. // Phys. Rev. Lett., 1981, vol. 46, p. 1461.
17. Guyer R.A., Miller M.D. // Phys. Rev. B, 1982, vol. 25, p. 5749.
18. Alikacem N., Sprague D.T., Hallock R.B. // Phys. Rev. Lett., 1991, vol. 67, p. 2501.
19. Alikacem N., Hallock R.B., Higley R.H., Sprague D.T. // J. Low Temp. Phys., 1992, vol. 87, p. 279.
20. Anderson R.H., Miller M.D. // J. Low Temp. Phys., 1999, vol. 116, p. 85.
21. Miller M.D., Nosanow L.H. // J. Low Temp. Phys., 1978, vol. 32, p. 145.
22. Dann M., Nyeki J., Cowan B., Saunders J. // J. Low Temp. Phys., 1998, vol. 110, p. 627.

Властивості тонких надплинних плівок ^3He - ^4He

Р.Г.Андерсон, М.Д.Міллер

Вашингтонський державний університет, фізичний факультет,
Пуллман, WA 99164-2814, США

Отримано 11 серпня 2000 р.

Тонкі плівки ^3He - ^4He є прикладом сильно взаємодіючих, квазідвовимірних, ферміонно-бозонних змішаних систем. Властивості змішаних систем можуть бути керовані зміною підкладки або товщини плівки ^4He . У цій статті ми обговорюємо основний стан і магнітний основний стан підсистеми ^3He , а також взаємодії між збудженнями надплинної плівки ^4He з одночастинковими збудженнями адсорбованого ^3He . Основний стан системи ^3He обчислюємо, використовуючи модель для ефективної взаємодії ^3He - ^3He у статичній плівці ^4He , яка явно включає ефективну взаємодію, зумовлену обміном віртуальними плівковими збудженнями (ріпплонами). Ця остання ефективна взаємодія оцінюється в наближенні хаотичних фаз, і показано, що вона не є здатна спричиняти самозв'язаність системи ^3He . З вимірювань намагніченості, третього звуку і питомої теплоємності ми обговорюємо свідчення того, що перший поперечний збуджений стан ^3He заповнюється раніше від завершення моношару.

Ключові слова: надплинні плівки, суміші ^3He - ^4He , третій звук, ріпплони

PACS: 67.70.+n, 67.60.Fp, 64.30.+t